

# Application of Nanofluids in Minimum Quantity Lubrication Grinding

BIN SHEN,<sup>1</sup> ALBERT J. SHIH,<sup>1</sup> and SIMON C. TUNG<sup>2</sup>

<sup>1</sup>Department of Mechanical Engineering

University of Michigan

Ann Arbor, MI 48109, USA

<sup>2</sup>Chemical and Environmental Science Lab

General Motors Research and Development Center

Warren, MI 48090, USA

*This research investigated the wheel wear and tribological characteristics in wet, dry, and minimum quantity lubrication (MQL) grinding of cast iron. Water-based Al<sub>2</sub>O<sub>3</sub> and diamond nanofluids were applied in the MQL grinding process and the grinding results were compared with those of pure water. During the nanofluid MQL grinding, a dense and hard slurry layer was formed on the wheel surface and could benefit the grinding performance. Experimental results showed that G-ratio, defined as the volume of material removed per unit volume of grinding wheel wear, could be improved with high-concentration nanofluids. Nanofluids showed the benefits of reducing grinding forces, improving surface roughness, and preventing workpiece burning. Compared to dry grinding, MQL grinding could significantly reduce the grinding temperature.*

## KEY WORDS

Grinding; Minimum Quantity Lubrication (MQL); Nanofluids; Abrasive Wear; Thermal Analysis

## INTRODUCTION

Grinding is widely used as the finishing machining process for components that require smooth surfaces and precise tolerances. A large volume of grinding fluid is most commonly used to flood the grinding zone, hoping to achieve tangible productivity targets while often neglecting the seemingly less tangible environmental and safety hazards. In addition, the inherent high cost of disposal or recycling of the grinding fluid becomes another major concern, especially as the environmental regulations get stricter. Minimizing the quantity of cutting fluid is desirable in grinding.

MQL is to supply a minute quantity of cooling lubricant medium to the contact point or to the zone so that the applied amount of grinding fluid can be reduced tremendously while maintaining the cooling and lubrication effects that are lost in

dry machining. Although MQL is widely applied in the cutting process such as turning, milling, and drilling, MQL grinding is still a relatively new research area. In previous research (Baheti, et al. (1); Hafenbraedl and Malkin (2)), the performance of MQL grinding using non-hazardous ester oil was evaluated relative to conventional 5% soluble oil as well as dry grinding for straight surface grinding and internal cylindrical grinding in terms of specific energy, surface roughness, wheel wear, and cooling. Experimental results showed that MQL provided effective lubrication but insufficient workpiece cooling with conventional abrasive wheels. MQL grinding has also been studied in Europe with similar conclusions (Brinksmeier, et al. (3)) regarding workpiece cooling.

The goal of this research is to study the wheel wear and tribological phenomena in MQL grinding. The fluid is a key technical area that can enable the success of MQL grinding processes. Nanofluids for grinding are investigated in this study. Nanofluids are engineered by dispersing nanometer-size solid particles in traditional heat transfer fluids to change their thermal and tribology properties. The effective thermal conductivity of ethylene glycol can be improved by up to 40% through the dispersion of 0.3 vol% Cu nanoparticles (Choi, et al. (4)). Carbon nanotubes (CNT) can yield an even larger increase in thermal conductivity (up to a 150% increase in conductivity of oil at approximately 1 vol% CNT; Choi, et al. (5); Lockwood, et al. (6)). For convection heat transfer, in the laminar flow regime the local heat transfer coefficient can be increased by 47% for a water-based nanofluid containing 1.6 vol% Al<sub>2</sub>O<sub>3</sub> nanoparticles (Wen and Ding (7)), while in the turbulent flow regime, the Nusselt number of the nanofluid is increased more than 39% for the nanofluid with 2 vol% of Cu nanoparticles (Xuan and Roetzel (8); Xuan and Li (9)). Another study of Al<sub>2</sub>O<sub>3</sub> nanoparticles in water has shown the temperature-dependent behavior of nanofluids (Das, et al. (10)), which indicates that nanofluids could be particularly attractive for applications at elevated temperatures.

In this paper, grinding of cast iron under different cooling lubrication conditions including the wet (flood cooling), dry, and MQL was studied. Water-based Al<sub>2</sub>O<sub>3</sub> and diamond nanofluids were applied in MQL grinding. Grinding performance was investigated

and compared in terms of grinding force, wheel wear ratio, surface roughness, and grinding temperature.

## EXPERIMENTAL SETUP

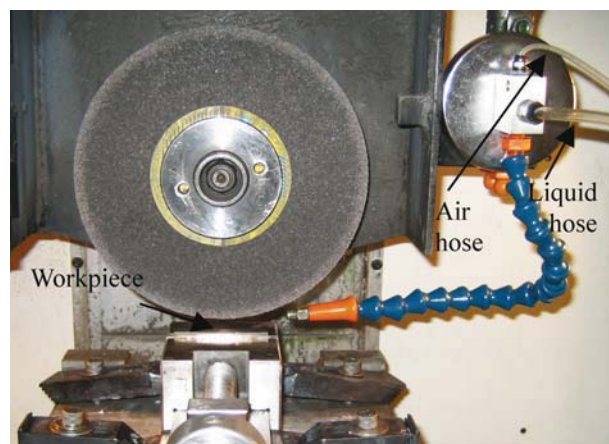
The grinding experiments were conducted in an instrumented Chevalier Model Smart-B818 surface grinding machine. The setup of the grinding experiment is shown in Fig. 1. An MQL fluid delivery system made by AMCOL was used. In this system, a biaxial hose is used to independently transport liquid and air to the point of use and then the liquid is surrounded with air (coaxial) and propelled onto the tool or workpiece by air pulse. A vitreous bond grey aluminum oxide grinding wheel (Saint-Gobain/Norton 32A46-HVBEP) with 508- $\mu\text{m}$  average abrasive size was used. The size of the grinding wheel is about 169 mm in diameter and 12.7 mm in width. The work material is Dura-Bar 100-70-02 ductile iron. This material has 3.5–3.9% carbon content, 50 Rockwell C hardness, 63 W/m·K thermal conductivity, and  $1.63 \times 10^{-7} \text{ m}^2/\text{s}$  thermal diffusivity. The width and length of the workpiece surface for grinding are 6.5 mm and 57.5 mm, respectively.

The surface speed of the wheel and the down feed were set to be 30 m/s and 10  $\mu\text{m}$ , respectively. The grinding was conducted by traversing the wheel across the workpiece at 2400 mm/min table speed in one direction. The grinding wheel was dressed at 10  $\mu\text{m}$  down feed, 500 mm/min traverse speed, and a  $-0.4$  speed ratio using a rotary diamond disk.

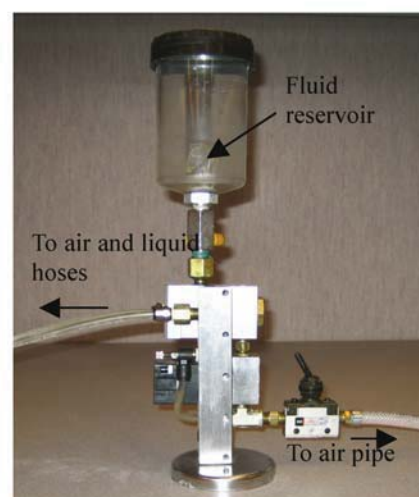
The normal and tangential grinding forces were measured using a Kistler Model 9257A piezoelectric dynamometer. The grinding temperatures were measured by the embedded thermocouple method, as seen in Fig. 1c. The temperature and grinding force data were collected at 5 kHz sampling rate. After each grinding pass, the workpiece was allowed to cool to the initial temperature before the next pass was taken.

The wheel wear measurement method is the same as described in Shih, et al. (11). The wheel is 12.7 mm wide, which is wider than the 6.5-mm width of the part. A worn groove is generated on the wheel surface after grinding. A hard plastic part was ground to produce a replica of the worn grinding wheel. A Taylor Hobson Talysurf profilometer was used to measure the depth of wheel wear on the replica. Each G-ratio grinding test had to wear out at least 6  $\mu\text{m}$  of the wheel to ensure the accuracy of the G-ratio. The same profilometer was used to measure the surface roughness of the ground surfaces. Three measurement traces parallel and perpendicular to the grinding direction were measured. The average of the three arithmetic average surface roughness ( $R_a$ ) measurements along and across the grinding direction was used to represent the roughness of a ground surface.

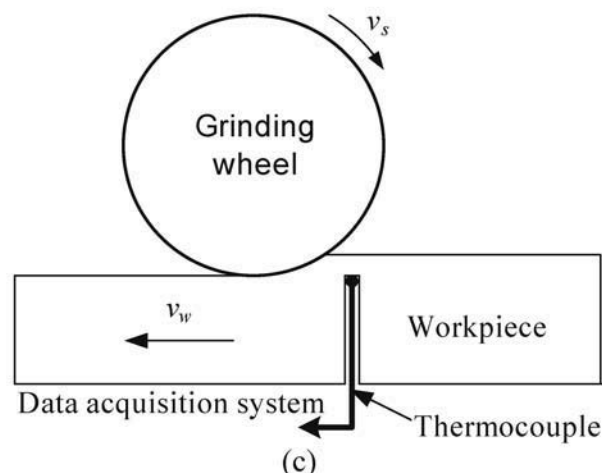
Four types of fluids were used in grinding tests, water-based Cimtech 500 (Milacron, Cincinnati, OH) synthetic grinding fluid at 5 vol% concentration, pure water, water-based  $\text{Al}_2\text{O}_3$  nanofluids, and water-based diamond nanofluids. The  $\text{Al}_2\text{O}_3$  nanofluids were prepared by dispersing 40 nm  $\text{Al}_2\text{O}_3$  nanoparticles (Nova-Centrix, Austin, Texas) in the deionized water. Three volume fractions of  $\text{Al}_2\text{O}_3$  nanofluids at 1.0%, 2.5%, and 4.0% were tested. The 4.0 vol% is already on the high side of concentration for  $\text{Al}_2\text{O}_3$  nanofluids because of the noted increase in vis-



(a)



(b)



(c)

Fig. 1—Experimental setup: (a) overview of the setup, (b) MQL fluid delivery device, and (c) schematic drawing of grinding temperature measurement.

cosity. Two diamond nanofluids samples are provided by Warren/Amplex Superabrasives of Saint-Gobain. Both samples are formulated to have a weight fraction of 250 carats/1000 mL, which have an equivalent volume fraction of 1.5% diamond. One sample

contains 200-nm carbon-coated diamonds and the other contains 100 nm non-coated mono-crystalline diamonds. For wet grinding with flood cooling, Cimtech 500 synthetic grinding fluid at 5 vol% concentration was used and the flow rate was measured as 5400 mL/min. For MQL grinding, the testing flow rate was set at 5 mL/min, except in the grinding temperature test, and different flow rates (5, 15, and 30 mL/min) were examined.

## EXPERIMENTAL RESULTS

### Fluid Thermal Conductivity

Before applying grinding fluid, their thermal conductivities were measured by the transient hot wire method (Nagasaka and Nagashima (12); Batty, et al. (13)). The thermal conductivity of fluids involved are all measured at room temperature and summarized in Table 1. The thermal conductivity of ethylene glycol and pure water were measured as 0.252 and 0.603 W/m-K, respectively, which are comparable to the reference values (0.250 W/m-K for ethylene glycol and 0.606 W/m-K for pure water) in Incropera and DeWitt (14). All the nanofluids show some enhancement in the thermal conductivity.  $Al_2O_3$  nanofluids have a thermal conductivity enhancement of 7%, 11%, and 15% for 1.0%, 2.5%, and 4.0% volume fraction concentration, respectively. Diamond nanofluids at 1.5 vol% have a thermal conductivity enhancement of 6% for 200-nm carbon-coated diamond and 10% for 100-nm non-coated diamond. The 5% concentration Cimtech 500 synthetic grinding fluid causes the thermal conductivity to drop to 0.593 W/m-K.

### Grinding Forces

The specific grinding forces, which are defined as the forces divided by the width of grinding, vs. passes are shown in Figs. 2 and 3. These forces are the average values in each grinding pass. The grinding forces for every five passes are plotted. As shown in Fig. 2, flood cooling and MQL grinding using Cimtech 500 generates similar normal and tangential forces during the entire process. These forces are lower than MQL grinding using pure water, which is expected because of the better lubricating properties of Cimtech 500 cutting fluid. Dry grinding without lubrication generates the highest forces. On the other hand, the forces increase

TABLE 1—FLUIDS THERMAL CONDUCTIVITY

Fluids	Thermal Conductivity (W/m-K)	Thermal Conductivity Enhancement
Ethylene glycol	0.252	—
Deionized water	0.603	—
Cimtech 500 synthetic fluid (5%)	0.593	—
$Al_2O_3$ nanofluids (40 nm diameter)		
1.0 vol%	0.645	7%
2.5 vol%	0.670	11%
4.0 vol%	0.693	5%
Diamond nanofluids (200 nm carbon coated)		
1.5 vol%	0.654	6%
Diamond nanofluids (100 nm non-coated) 1.5 vol%	0.684	10%

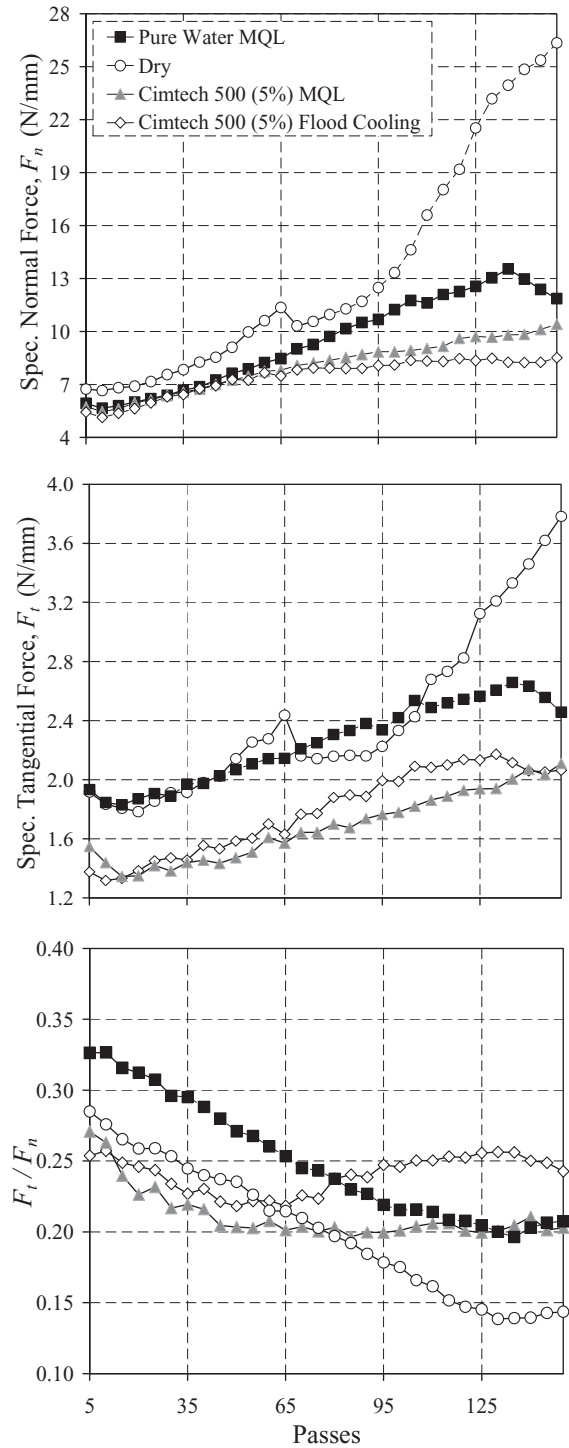


Fig. 2—Specific grinding forces and force ratio for wet, dry, and MQL grinding using Cimtech 500 and pure water.

with the number of passes, which is attributed to the wheel wear. Notice that the forces for dry grinding increase exponentially after 110 passes. These large forces generate excessive heat and lead to visible burning of the workpiece, which can be identified by discoloration on the ground workpiece surface.

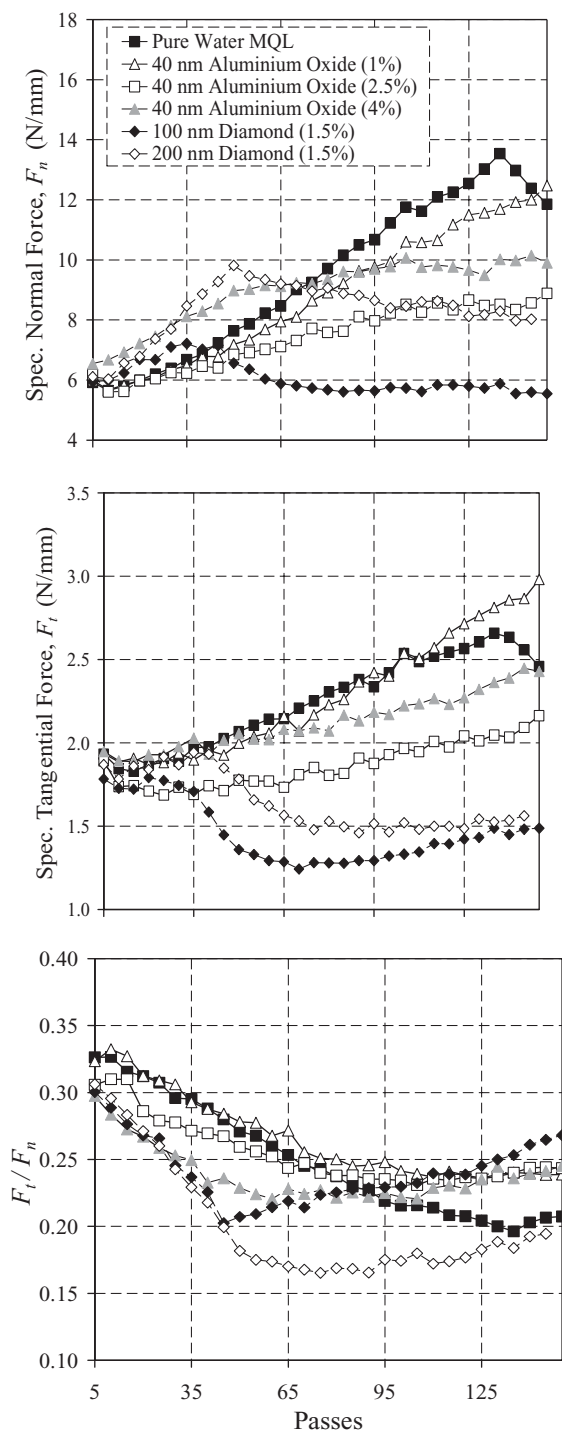


Fig. 3—Specific grinding forces and force ratio for water-based nanofluids.

MQL grinding force results using pure water (considered as the datum) and water-based nanofluids are compared in Fig. 3. In the beginning (before 35 passes), all the forces are comparable. With increasing passes, MQL grinding using different fluids exhibits different performance. For  $Al_2O_3$  nanofluids, at 1.0 vol% low concentration, the grinding forces increase progressively, which is similar to the case of pure water. At higher concentration (2.5 and

4.0 vol%), the grinding forces remain flat after increasing in the beginning. This may be due to the hard and dense slurry layer observed on the grinding wheel. However, compared with  $Al_2O_3$  nanofluid of 2.5 vol%, the one with 4.0 vol% gives much higher forces. The possible explanation is that the high concentration of  $Al_2O_3$  (4.0 vol%) leads to excessive loading of the vitreous bond grinding wheel, resulting in higher grinding forces.

For diamond nanofluids, the grinding forces become flat after about 45 passes. Again, the slurry layer is readily observed when using 200-nm carbon-coated diamond nanofluids but not for 100-nm non-coated diamond nanofluids. Intense loading on the wheel is likely why the grinding forces are higher with 200-nm carbon-coated diamond nanofluid than with 100-nm non-coated diamond nanofluid. In general, the slurry layer can reduce the grinding forces by reducing the wheel wear, which is supported by the G-ratio measurement results.

The force ratio  $F_t/F_n$  indicates the combination of abrasive cutting and friction between the wear flats and the workpiece. In all the experiments, this ratio decreases from the beginning and then reaches a relatively steady-state value. As shown in Fig. 2, the force ratio is 0.15 for dry, 0.2 for pure water and Cimtech 500 MQL, and 0.25 for Cimtech 500 flood cooling grinding. For nanofluid MQL grinding, as shown in Fig. 3, the force ratio is 0.25 for all three  $Al_2O_3$ -based nanofluids and about 0.27 and 0.2 for the 100- and 200-nm diamond nanofluids grinding, respectively. The initial drop is probably due to the rise of workpiece temperature during grinding. In dry grinding, the ratio is very low, which is attributed to the workpiece burning and associated phase changes (Malkin (15)).

The specific tangential versus specific normal force for all grinding conditions is illustrated in Fig. 4. For given grinding conditions,

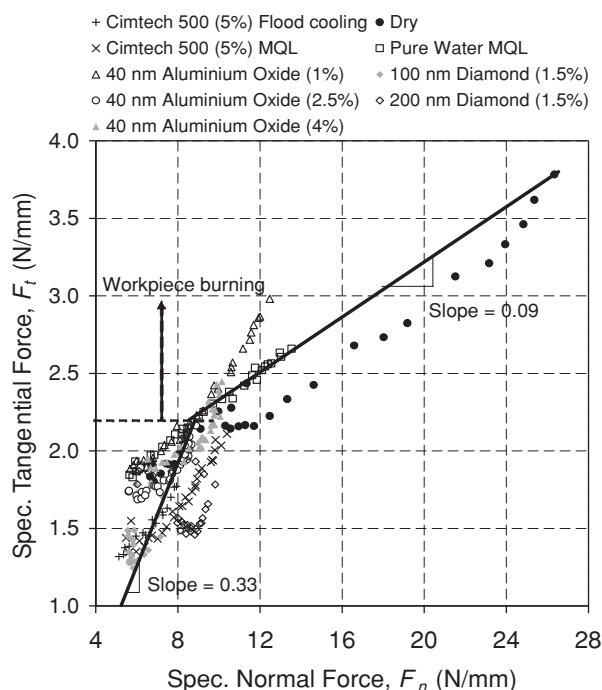


Fig. 4—Specific tangential force vs. specific normal force.



a plot of the tangential versus the normal force component per unit width should yield a straight line with a slope equal to the friction coefficient between the wear flats and the workpiece. According to Malkin's analysis (Malkin (15)), above the burn limit, the slope gets steeper, which suggests a decrease in friction coefficient associated with workpiece burn. The phase changes and the formation of oxides on the cast iron workpiece cause the reduction in friction coefficient. This change in the slope or the friction coefficient is also observed in this study. As shown in Fig. 4, the specific tangential grinding force of about 2.2 N/mm is the transition point for grinding burn and change of slope. This corresponds to a specific energy of 165 J/mm<sup>3</sup>, which is a little higher than 135 J/mm<sup>3</sup> burning limit for low carbon and low alloy steels (Malkin (15)).

Linear curve fitting was applied to data points above and below the 2.2 N/mm specific tangential grinding force. In the absence of workpiece burn, below the specific tangential grinding force of 2.2 N/mm, the slope is 0.33, which implies a friction coefficient of 0.33 between the wear flats and the workpiece. With grinding burn, the slope is much lower, 0.09. This indicates a much smaller friction coefficient beyond this grinding burn point. This observation is consistent with the findings in previous grinding studies (Malkin (15)). Workpiece burning, evidenced by visible discoloration, is apparent in three grinding conditions: dry, pure water MQL, and 1.0 vol% Al<sub>2</sub>O<sub>3</sub> nanofluids MQL grinding. For dry grinding, except for several initial passes, most of the data points are above the burn limit. This has also been observed on the discoloration of the ground surface. The experimental observations of discoloration match the burn limit prediction in Fig. 4. Slight discoloration was observed for pure water and 1.0 vol% Al<sub>2</sub>O<sub>3</sub> nanofluids MQL grinding. As shown in Fig. 4, some data from these experiments also locate above the burn limit. For pure water, the lack of lubricity contributes to the workpiece burning. For 1.0 vol% Al<sub>2</sub>O<sub>3</sub> nanofluid, it is likely attributed to the relatively high grinding force than the other nanofluids, as shown in Fig. 3. No burning marks were observed for 2.5 vol% Al<sub>2</sub>O<sub>3</sub> nanofluids, diamond nanofluids,

flood cooling, and MQL grinding with Cimtech 500 as the specific tangential forces in these experiments are all below 2.2 N/mm.

### G-ratio

G-ratio is defined as the volume of work material removed divided by the volume of wheel wear. A high G-ratio indicates low wheel wear rate. Nanofluid MQL grinding generally exhibits high G-ratio, ranging from 16 to 33, as shown in Fig. 5. Flood cooling and MQL grinding using Cimtech 500 provides a similar G-ratios, about 17. Dry grinding exhibits the worst wheel wear, i.e., the lowest G-ratio, about 12, while MQL using pure water has only a slightly higher G-ratio than that of dry grinding.

For MQL grinding with Al<sub>2</sub>O<sub>3</sub> nanofluids the G-ratio increases with the increasing volume fractions of Al<sub>2</sub>O<sub>3</sub> nanoparticles. The two highest G-ratio results are observed in MQL grinding with 2.5 and 4.0 vol% Al<sub>2</sub>O<sub>3</sub> nanofluids. This is attributed to the formation of the slurry layer, which can protect the grinding wheel from grain/bond fracture. High-concentration nanofluid has better protection and improves the G-ratio. The slurry layer is not observed in MQL grinding with 1.0 vol% Al<sub>2</sub>O<sub>3</sub> nanofluid, which has a low G-ratio. In early research by Komanduri and Reed (16), it was found that a thin slurry layer of silicon carbide on the wheel surface can protect the bonding material from thermal and/or mechanical degradation or damage, thereby causing a high G-ratio. This research further validates this observation.

For MQL grinding with diamond nanofluids, the same phenomenon of slurry formation and high G-ratio was observed in the 200-nm diamond nanofluid. For the 100-nm diamond nanofluid, no slurry layer was observed and the G-ratio is lower than that of the 200-nm diamond nanofluids. Compared to the 100-nm diamond nanofluid, it should also be noted that the 200-nm diamond nanofluid is more viscous and more ready to form the slurry layer.

### Surface Roughness

The surface roughness ( $R_a$ ) of the ground workpiece is presented in Fig. 6. Flood cooling has the best surface finish (lowest

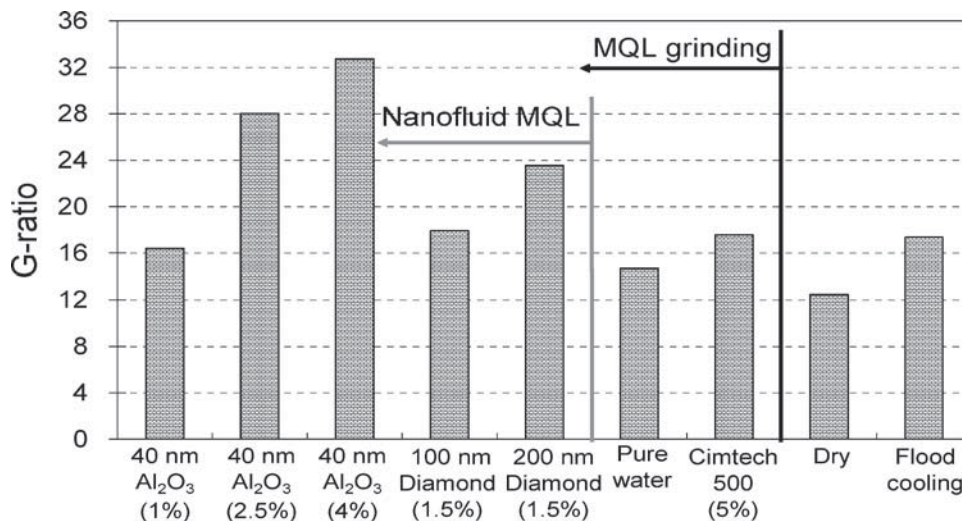


Fig. 5—G-ratio results.

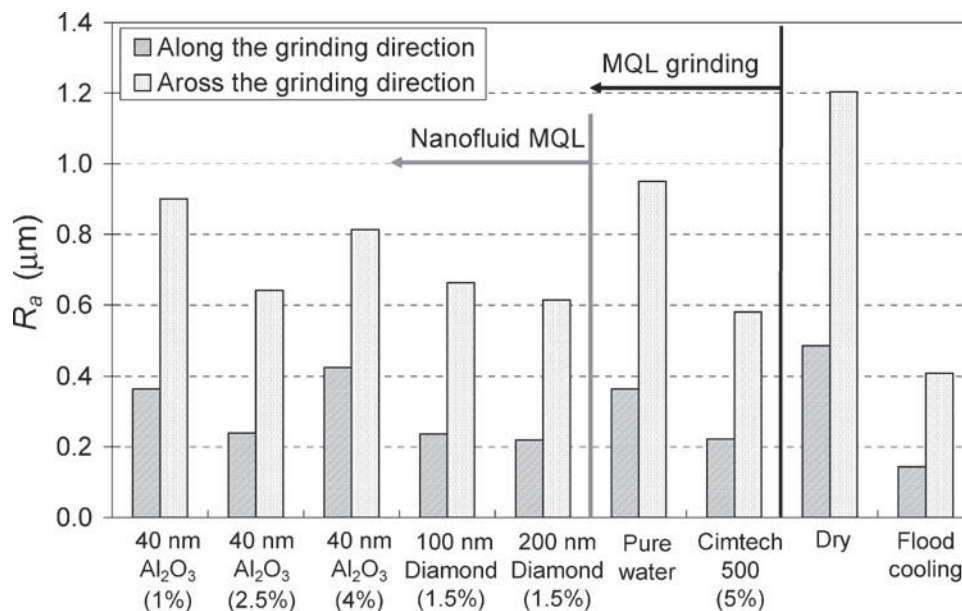


Fig. 6—Surface roughness results.

surface roughness). In general, MQL grinding using nanofluids has a better surface finish than pure water but worse than the flood cooling and MQL grinding using Cimtech 500. Cimtech 500 synthetic grinding fluid provides good lubrication, while pure water has a poor lubricating capability. The flood cooling also provides efficient chip flushing. The fact that the nanofluids outperform the pure water can be partly due to the reduction in grinding forces and friction. Dry grinding has the worst surface finish, which is expected.

For  $\text{Al}_2\text{O}_3$  nanofluids, 2.5 vol% has better surface roughness than that of 1.0 and 4.0 vol%. The 2.5 vol%  $\text{Al}_2\text{O}_3$  nanofluid has the lowest specific tangential grinding forces (see Fig. 3) among the three. The 4.0 vol%  $\text{Al}_2\text{O}_3$  nanofluid has lower specific tangential grinding forces than the 1.0 vol%  $\text{Al}_2\text{O}_3$  nanofluid. As a result, the 4.0 vol%  $\text{Al}_2\text{O}_3$  nanofluid has a better surface finish across the grinding direction. However, along the grinding direction, it has a worse surface finish than the 1.0 vol%  $\text{Al}_2\text{O}_3$  nanofluid. This is likely due to the thicker slurry layer in 4.0 vol%  $\text{Al}_2\text{O}_3$  nanofluid MQL grinding, which may scratch the workpiece along the grinding direction.

The 200-nm coated diamond nanofluids have a slightly better surface finish than the 100-nm non-coated diamond nanofluid. Although the former has slightly higher tangential forces, it has a lower force ratio (friction coefficient). In general, diamond nanofluids perform better than  $\text{Al}_2\text{O}_3$  nanofluids in terms of surface roughness due to the lower specific tangential grinding forces, as seen in Fig. 3.

### Grinding Temperature

The comparison of wet, dry, and MQL grinding temperature at the workpiece surface was plotted in Fig. 7. Flood cooling has the lowest temperature and dry grinding has the highest, which is expected. In Fig. 7, all the MQL grinding experiments have the same flow rate (5 mL/min). By applying MQL, the peak temperature

is about 100–150°C lower than that in dry grinding. This is due to both the cooling and the lubrication effects of the fluids provided by MQL, as lubrication reduces the cutting forces and cutting energy, while convection heat transfer and/or boiling carries away some of the heat.

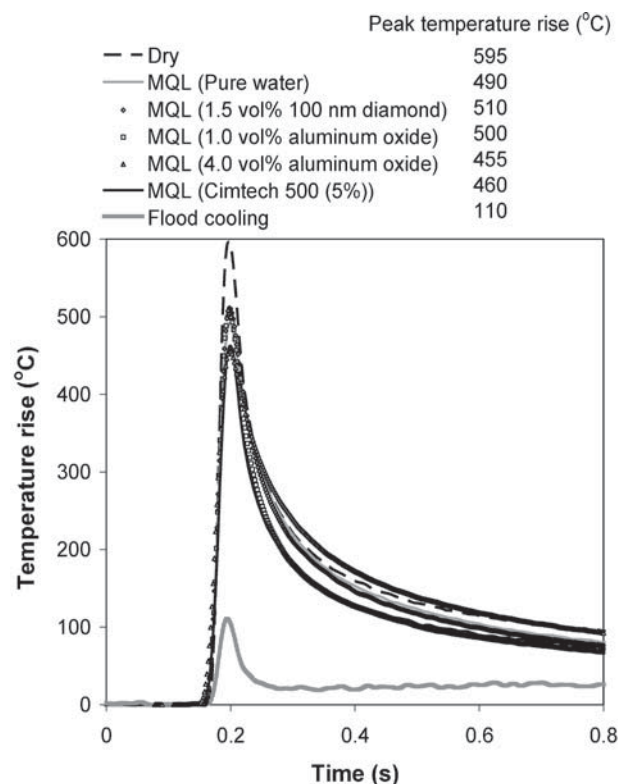


Fig. 7—Comparison of wet, dry, and MQL grinding temperature at the workpiece surface (5 mL/min flow rate for MQL grinding).

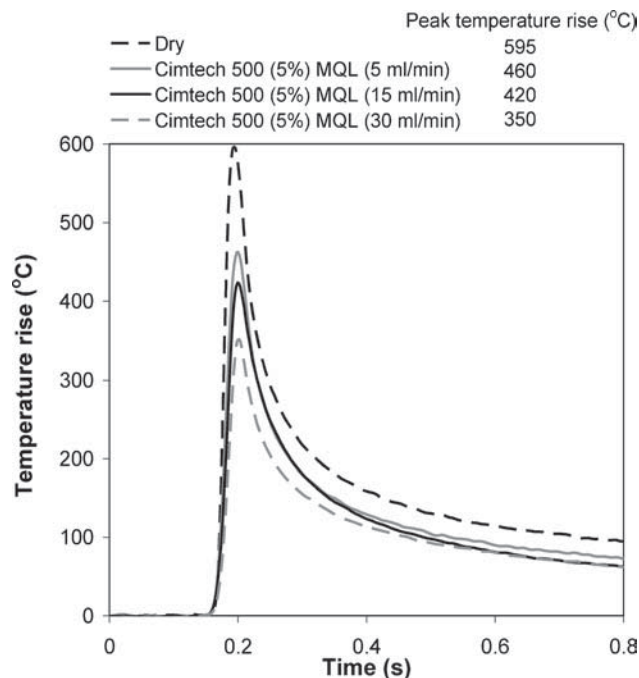


Fig. 8—Fluid flow rate effects on grinding temperature at the workpiece surface.

There is no significant difference in grinding temperature among the experiments using different types of fluids for MQL grinding. The Cimtech 500 synthetic grinding fluid has slightly lower grinding temperature. This is probably attributed to the better lubrication properties of Cimtech 500 synthetic grinding fluid. The 4.0 vol% aluminum oxide nanofluids also have a slightly lower workpiece surface grinding temperature. This is probably due to the dense slurry layer formed during grinding, which may cause more heat to enter the grinding wheel than the workpiece.

Further investigation was conducted on the flow rate effects, as shown in Fig. 8. Larger MQL flow rate leads to the lower grinding temperature. Increasing the flow rate from 5 to 30 mL/min, the peak grinding temperature was reduced by about 100°C, which is 250°C lower than that in completely dry grinding. This also indicates that the flow rate setting is a very critical factor in MQL grinding. By increasing the MQL flow rate, it is possible to achieve the desired cooling effects.

### CONCLUDING REMARKS

Grinding of cast iron under different lubrication conditions was studied. Grinding performance was investigated and compared in terms of grinding forces, G-ratio, surface roughness, and grinding temperature. Dispersion of solid particles was found to play an important role, especially when a slurry layer was formed. The slurry layer generated a higher G-ratio (less wheel wear), smaller grinding forces, and better surface finish. To elucidate how the slurry layer forms and how the dispersed solid particles and the slurry layer affect the grinding performance, further research is needed.

The preliminary study of MQL grinding showed that it could significantly reduce the grinding temperature compared to dry

grinding. However, there is no significant difference in grinding temperature when using nanofluids. This is probably because the amount of the nanofluids applied in MQL grinding is too small to make any difference even though they have better heat transfer and thermal conductivity. In addition, convection or sometimes boiling is the dominant cooling phenomenon in grinding processes rather than conduction. Therefore, further investigation on the convection heat transfer and boiling of nanofluids is needed to better understand the cooling advantages provided by nanofluids MQL grinding process.

This study also quantitatively demonstrated that the flow rate was very important in MQL grinding and it was possible to achieve the desired cooling effects by increasing the amount of fluids applied in MQL grinding. Further research is ongoing in order to optimize the MQL grinding process.

### ACKNOWLEDGMENTS

This research is sponsored by the National Science Foundation DMII Grant #0422947 and General Motors Research Discovery Project. Supports from Saint-Gobain Abrasives, AMCOL Corporation, and NovaCentrix Corp. are greatly appreciated. The authors would like to thank Stephen Malkin, Eric Schneider, Guoxian Xiao, Changsheng Guo, Stephen Choi, and Alan Rakouskas for their technical assistance and advice.

### REFERENCES

- (1) Baheti, U., Guo, C. and Malkin, S. (1998), "Environmentally Conscious Cooling and Lubrication for Grinding," Proc. CIRP Int. Seminar on Improving Machine Tool Performance, San Sebastian, Spain, pp 643-654.
- (2) Hafenbraedl, D. and Malkin, S. (2000), "Environmentally-Conscious Minimum Quantity Lubrication (MQL) for Internal Cylindrical Grinding," *Trans. NAMRI/SME*, **28**, pp 149-154.
- (3) Brinksmeier, E., Brockhoff, T. and Walter, A. (1997), "Minimalmengekülschmierung und Trockenbearbeitung beim Schleifen," *Haerterei-Technische Mitteilungen*, **52**, pp 166-170.
- (4) Choi, S. U. S., Li, S., Yu, W. and Thompson, L. J. (2001), "Anomalous Increased Effective Thermal Conductivities of Ethylene Glycol-Based Nanofluids Containing Copper Nanoparticles," *Applied Physics Letters*, **78**, 6, pp 718-720.
- (5) Choi, S. U. S., Zhang, Z. G., Yu, W., Lockwood, F. E. and Grulke, E. A. (2001), "Anomalous Thermal Conductivity Enhancement in Nanotube Suspensions," *Applied Physics Letters*, **79**, pp 2252-2254.
- (6) Lockwood, F. E., Zhang, Z. G., Forbus, T. R., Choi, S. U. S., Yang, Y., and Grulke, E. A. (2005), "The Current Development on Nanofluid Research," SAE 2005 World Congress, Detroit, MI, SAE International.
- (7) Wen, D. and Ding, Y. (2004), "Experimental Investigation into Convective Heat Transfer of Nanofluids at the Entrance Region under Laminar Flow Conditions," *International Journal of Heat and Mass Transfer*, **47**, 24, pp 5181-5188.
- (8) Xuan, Y. M. and Roetzel, W. (2000), "Conceptions for Heat Transfer Correlation of Nanofluids," *International Journal of Heat and Mass Transfer*, **43**, 19, pp 3701-3707.
- (9) Xuan, Y. M. and Li, Q. (2003), "Investigation on Convective Heat Transfer and Flow Features of Nanofluids," *Journal of Heat Transfer*, **125**, 1, pp 151-155.
- (10) Das, S. K., Putra, N., Thiesen, R. and Roetzel, W. (2003), "Temperature Dependence of Thermal Conductivity Enhancement for Nanofluids," *Journal of Heat Transfer*, **125**, 4, pp 567-574.
- (11) Shih, A. J., Curry, A. C., Scattergood, R. O., Yonushonis, T. M., Gust, D. J., Grant, M. B., McSpadden, S. B. and Watkins T. (2003), "Cost-Effective Grinding of Zirconia Using the Dense Vitreous Bond Silicon Carbide Wheel," *Journal of Manufacturing Science and Engineering*, **125**, 2, pp 297-303.
- (12) Nagasaka, Y. and Nagashima, A. (1981), "Absolute Measurement of the Thermal Conductivity of Electrically Conducting Liquids by the Transient Hot-Wire Method," *J. Physics E: Sci. Instruments*, **14**, 12, pp 1435-144.

- (13) Batty, W. J., O'Callaghan, P. W. and Probert, S. D. (1984), "Assessment of the Thermal-Probe Technique for Rapid, Accurate Measurements of Effective Thermal Conductivities," *Applied Energy*, **16**, 2, pp 83-113.
- (14) Incropera, F. P. and DeWitt, D. P. (2001), *Fundamentals of Heat and Mass Transfer*, 5th Edition, John Wiley & Sons Inc., NJ.
- (15) Malkin, S. (1989), *Grinding Technology: Theory and Applications of Machining with Abrasives*, Halsted Press, New York.
- (16) Komanduri, R. and Reed, W. R. (1980), "New Technique of Dressing and Conditioning Resin Bonded Superabrasive Grinding Wheels," *Annals CIRP*, **29**, 1, pp 239-243.